Structure-Function Analysis of Lyn Kinase Association with Lipid Rafts and Initiation of Early Signaling Events after Fcε Receptor I Aggregation

MARTINA KOVÁŘOVÁ,[1,2] PAVEL TOLAR,[1] RAMACHANDRAN ARUDCHANDRAN,[2]
LUBICA DRÁBEROVÁ,[1] JUAN RIVERA,[2]* AND PETR DRÁBER[1]

*Institute of Molecular Genetics, Academy of Sciences of the Czech Republic, 14220 Prague, Czech Republic,[1] and
Molecular Inflammation Section, National Institute of Arthritis and Musculoskeletal and Skin Diseases,
National Institutes of Health, Bethesda, Maryland 20892-1820[2]*

The first step in immunoreceptor signaling is represented by ligand-dependent receptor aggregation, followed by receptor phosphorylation mediated by tyrosine kinases of the Src family. Recently, sphingolipid- and cholesterol-rich plasma membrane microdomains, called lipid rafts, have been identified and proposed to function as platforms where signal transduction molecules may interact with the aggregated immunoreceptors. Here we show that aggregation of the receptors with high affinity for immunoglobulin E (FcεRI) in mast cells is accompanied by a co-redistribution of the Src family kinase Lyn. The co-redistribution requires Lyn dual fatty acylation, Src homology 2 (SH2) and/or SH3 domains, and Lyn kinase activity, in *cis* or in *trans*. Palmitoylation site-mutated Lyn, which is anchored to the plasma membrane but exhibits reduced sublocalization into lipid rafts, initiates the tyrosine phosphorylation of FcεRI subunits, Syk protein tyrosine kinase, and the linker for activation of T cells, along with an increase in the concentration of intracellular Ca^{2+}. However, Lyn mutated in both the palmitoylation and myristoylation sites does not anchor to the plasma membrane and is incapable of initiating FcεRI phosphorylation and early signaling events. These data, together with our finding that a constitutively tyrosine-phosphorylated FcεRI does not exhibit an increased association with lipid rafts, suggest that FcεRI phosphorylation and early activation events can be initiated outside of lipid rafts.

The high-affinity immunoglobulin E (IgE) receptor (FcεRI)-mediated activation of mast cells and basophils triggers a cascade of intracellular biochemical events that ultimately lead to the secretion of preformed pharmacological agents and the transcription of cytokine genes. This process is initiated by aggregation of the receptor by means of multivalent antigen (Ag)-IgE complexes, followed by tyrosine phosphorylation of the receptor subunits by Src family protein tyrosine kinases (14, 31).

FcεRI has a tetrameric structure comprised of an IgE-binding α subunit, a β subunit, and a disulfide-bonded γ dimer (32). The β and γ subunits possess immunoreceptor tyrosine-based activation motifs (ITAMs), which are rapidly phosphorylated by protein tyrosine kinase Lyn. Tyrosine-phosphorylated ITAMs of the the γ subunits serve as novel binding sites for Src homology 2 (SH2) domains of Syk kinase (6, 22, 28), leading to phosphorylation and activation of Syk. Thereafter, a number of other signaling and adaptor molecules become phosphorylated and recruited into the regions of activated FcεRI/Syk complexes. These include PLCγ1 (26), the proto-oncogene product Vav (41), PKC-δ (18), and the linker for activation of T cells (LAT) (37, 52).

Detailed molecular mechanisms of the initial engagement of the Lyn kinase and FcεRI are not completely understood, but two different models have been proposed. One model, based

on protein-protein interactions, postulates that a small fraction of Lyn is constitutively associated with the β subunit of the FcεRI prior to activation. FcεRI aggregation effected by multivalent antigen-IgE complexes or by other means facilitates the transphosphorylation of one FcεRI by Lyn bound to a juxtaposed receptor (33). The tyrosine phosphorylation of β and γ subunits of FcεRI supports the recruitment of additional Lyn to β subunit and of the Syk kinase to γ subunits, promoting further propagation of the activation signal.

The alternative model postulates that the initial coupling of Lyn with aggregated FcεRI is mediated by protein-lipid interactions. According to this model, Lyn is anchored to the inner leaflet of the plasma membrane via myristate and palmitate chains that localize it in lipid rafts enriched in glycosphingolipids, cholesterol, and glycosylphosphatidylinositol-anchored proteins. These domains, which are also referred to as detergent-insoluble glycosphingolipid domains, have been found in numerous cell types (9, 40). Upon aggregation, the FcεRI rapidly translocates into lipid rafts, where it is phosphorylated by Lyn kinase (15, 39).

Although the model based on the sequestration of signal transduction molecules into lipid rafts is very attractive and was recently supported by analyses of activation via the T-cell receptor (51, 23, 29) and B-cell receptor (10), it is not completely clear how the receptor aggregation leads to its inclusion in lipid rafts and whether this is important for early activation events. For example, aggregation of FcεRI on rat basophilic leukemia (RBL) cells (a mast cell tumor analog) by divalent monoclonal antibodies (MAbs), which induce little visible re-

* Corresponding author. Mailing address: NIAMS/NIH, Building 10, Room 9N228, MSC 1820, Bethesda, MD 20892-1820. Phone: (301) 496-7592. Fax: (301) 402-0012. E-mail: juan_rivera@nih.gov.

ceptor aggregation, as determined by light and scanning electron microscopy (30), results in a cellular response similar to that caused by aggregation induced by a multivalent Ag that causes extensive FcεRI aggregation (42).

To investigate the localization of Lyn kinase and its functional consequences, we tagged Lyn with green fluorescense protein (GFP) and followed its distribution in RBL cells, mouse bone marrow-derived mast cells (BMMC), and BMMC from a mouse with a genetically disrupted Lyn gene (BMMC-Lyn$^{-/-}$) (19) before and after FcεRI engagement. Various Lyn-GFP constructs with defects in palmitoylation, myristoylation, or both acylation sites, as well as mutations in the SH1 and SH2/SH3 domains, and constitutively tyrosine-phosphorylated FcεRI were employed to determine the factors affecting the early stages of FcεRI-mediated activation. These experiments suggest that FcεRI phosphorylation and early activation events can be initiated outside of lipid rafts.

MATERIALS AND METHODS

Antibodies, reagents, and cell cultures. Mouse MAbs specific for Lyn, Syk, β subunit of FcεRI, 2,4,6-trinitrophenyl (TNP)-specific IgE (IGEL b4 1), and 2,4-dinitrophenyl (DNP)-specific IgE have been described previously (13, 35, 36, 45, 46). Rabbit polyclonal Ab specific for Syk, Lyn, LAT, GFP, and IgE were prepared by immunization with the recombinant fragments of Syk (2), Lyn (13), LAT, and GFP (unpublished) or IGEL b4 1 MAb, respectively. A chicken antibody to FcRγ has been described previously (45). Horseradish peroxidase (HRP)-conjugated mouse antiphosphotyrosine MAb PY-20, goat anti-mouse IgG, and goat anti-rabbit IgG were purchased from Transduction Laboratories. Antiphosphotyrosine MAb (4G10) and anti-Shc were obtained from Upstate Biotechnology, and anti-c-Src MAb (B 12) was from Santa Cruz Biotechnology. RBL-2H3 cells and their culture conditions have been described (11). RBL-2H3 cells defective in FcεRIγ and transfected with wild-type FcεRIγ (γwt) or with mutated FcεRIγ chain in which a threonine at position 52 was substituted for alanine (γT52A) have been described (45). BMMC and BMMC-Lyn$^{-/-}$ (19) were kindly provided by M. Hibbs (Ludwig Institute for Cancer Research, Melbourne, Australia).

DNA constructs, recombinant SFV, and infection. The Semliki Forest virus (SFV) gene expression system, pSFV1 and helper pSFV2, was purchased from Life Technologies. pSFV1 was further modified to contain a multiple cloning site and a GFP expression cassette as previously described (4). Lyn mutants were generated by PCR from cDNA encoding wild-type rat LynA and LynB (48).

In the primers described below, the mutation sites are marked by double lines, AvrII restriction sites by bold letters, and the optimized ribosome-binding sites by a single line. The following 5′ primers were used for the construction of wild-type LynA-GFP (LynA-WT) and wild-type LynB-GFP (LynB-WT): 1, 5′-AAA CCT AGG GCC ACC ATG GGA TGT ATT AAA TCA AAA AGG AAA GAC-3′ (5′Lyn-WT primer); 2, LynB in which Cys3 was replaced by Ala (LynB-CA), 5′-AAA CCT AGG GCC ACC ATG GGA GCT ATT AAA TCA AAA AGG AAA GAC-3′; 3, LynB in which Gly2 was replaced by Ala (LynB-GA), 5′-AAA CCT AGG GCC ACC ATG GCA TGT ATT AAA TCA AAA AGG AAA GAC-3′; and 4, LynB in which both Gly2 and Cys3 were replaced by Ala (LynB-GCA), 5′-AAA CCT AGG GCC ACC ATG GCA GCT ATT AAA TCA AAA AGG AAA GAC-3′. As a 3′ primer, the oligonucleotide 5′-AAA CCT AGG TGG CTG CTG CTG ATA CTG CCC TTC CGT GGC AGT GTA-3′ was used.

Unique domains of LynA (LynA-UNI) and LynB (LynB-UNI) were prepared by combining the 5′Lyn-WT primer and Lyn 3′ primer: 5′-AAA CCT AGG GTC CCC TTG CTC CTC TGG ATC TTT TGC-3′. For construction of LynA without a catalytic domain (LynA-SH2), the 5′Lyn-WT primer was combined with 3′ primer: 5′-AAA CCT AGG TTT CAC CAG CTT AAT GGA CTC CCG-3′.

The PCR-generated DNA fragments were digested with AvrII restriction enzyme and inserted into AvrII-digested pSFV1-EGFP (4). A construct with a mutation in the catalytic domain (LynB-CI) was prepared from Lyn CI (48). A schematic representation of the Lyn constructs used in this study is shown in Fig. 1. For all PCRs, the proofreading Pfu DNA polymerase (Stratagene) was used. Fidelity of all PCR products was confirmed by direct sequencing. Generation of SFV and infection of cells with recombinant viruses were done as described (4).
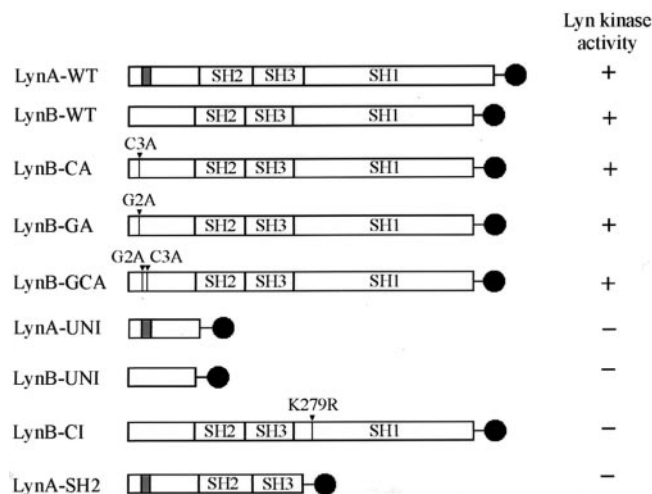

FIG. 1. Schematic representation of Lyn constructs. All constructs were tagged at the C terminus with enhanced GFP (solid circle). LynA-WT and LynB-WT are constructs with two forms of wild-type Lyn kinase that differ in a 20-amino-acid-long insert in the unique domain (shaded box). LynB-CA, LynB-GA, and LynB-GCA are constructs mutated in the palmitoylation, myristoylation, or both acylation sites, respectively. LynA-UNI and LynB-UNI contain only the N-terminal unique domains of LynA and LynB, respectively. LynB-CI is catalytically inactive Lyn B (mutation of Lys279 to Arg). LynA-SH2 is LynA without the catalytic domain. Arrows mark sites of introduced point mutations. The kinase activity of all Lyn constructs is indicated as full (+) and null (−) kinase activity.

SFV infectivity ranged from 60 to 90% for RBL-2H3 cells and 20 to 60% for BMMC and BMMC-Lyn$^{-/-}$.

Confocal microscopy. The cells were sensitized with biotinylated IgE (1.5 μg/ml) immediately after infection. After incubation for 3 h at 37°C, the cells were washed twice in buffered saline solution (BSS) containing 20 mM HEPES (pH 7.4), 135 mM NaCl, 5 mM KCl, 1.8 mM CaCl$_2$, 1 mM MgCl$_2$, 5.6 mM glucose, and 1 mg of bovine serum albumin (BSA) per ml and suspended at a concentration of 10^6 cells/ml in indocarbocyanine (Cy3)-conjugated streptavidin (Pierce; 2 μg/ml) in BSS/BSA. After 2 min at 37°C, the cells were washed in phosphate-buffered saline (PBS), transferred onto cover slips, pretreated with poly-L-lysine in PBS (Sigma; 100 μg/ml) in a 24-well plate, and centrifuged for 1 min at 200 × g. Attached cells were fixed with 4% paraformaldehyde for 15 min at room temperature, washed twice in PBS, dried in air, and mounted in ProLong antifade reagent (Molecular Probes). Control cells were fixed with paraformaldehyde before exposure to Cy3-streptavidin.

The confocal fluorescence images were taken using a Leica TCS NT/SP confocal system in conjunction with a Leica DM R microscope (Leica Microsystems). Achromatically corrected objective ×100 (NA 1.4) was used to simultaneously collect green and red images of the cells. Fluorescence bleedthrough was evaluated by separate excitation with blue (488 nm) or yellow (568 nm) laser lines (argon-krypton mix gas laser). Cross-correlation analysis of the co-redistribution of Lyn-GFP constructs with aggregated FcεRI complexes was carried out on equatorial images of individual cells using the quantification mode of the Leica TCS NT software (Leica Microsystems). The correlation coefficients were calculated from this analysis as described (38). These values were averaged for 12 to 16 cells from each sample for numerical comparison of the degree of co-redistribution.

Isolation of plasma membranes and lipid rafts. Cell membranes were isolated 4 h after infection. The cells were harvested and washed twice with ice-cold PBS, and 5 × 10^6 cells were resuspended in 500 μl of ice-cold homogenizing buffer (10 mM Tris-HCl [pH 8.0], 0.5 mM MgCl$_2$) containing protease inhibitors (1 mM phenylmethylsulfonyl fluoride [PMSF] plus 0.5 U of aprotinin and 0.5 U of leupeptin per ml). After 10 min of incubation on ice, the cells were homogenized by passing them 10 times through a 27-gauge needle, followed by an addition of 150 μl of tonicity restoration buffer (10 mM Tris-HCl [pH 8.0] 0.5 mM MgCl$_2$, 0.6 M NaCl). Insoluble material was removed by centrifugation, and the postnuclear supernatant was supplemented with 6.5 μl of 0.5 M EDTA and then centrifuged at 100,000 × g for 45 min. The membrane pellet was resuspended in

ice-cold 1% Triton X-100 lysis buffer (20 mM Tris-HCl [pH 8.0], 140 mM NaCl, 2 mM EDTA, 1 mM Na$_3$VO$_4$, 1 mM PMSF, and 0.5 U of aprotinin and 0.5 U of leupeptin per ml). After 20 min on ice, the insoluble material was removed by centrifugation for 10 min at 4°C at 10,000 × g, and the supernatant was used for further analysis.

Lipid rafts were isolated by sucrose density gradient ultracentrifugation as described (43). For analysis of density distribution of FcεRI and its aggregated forms as well as Lyn and Src kinases, the cells (2 × 10^7) were sensitized in suspension with ^{125}I-labeled TNP-specific IgE and activated or not as described in Results. The cells were lysed in 0.8 ml of lysis buffer containing 10 mM Tris-HCl (pH 8.0), 50 mM NaCl, 10 mM EDTA, 1 mM Na$_3$VO$_4$, 10 mM glycerophosphate, 1 mM PMSF, 0.5 U of aprotinin and 0.5 U of leupeptin per ml, and 0.06, 0.1, or 0.2% (vol/vol) Triton X-100. After 15 min, the lysate was homogenized by passing 10 times through a 27-gauge needle and adjusted to 40% (wt/vol) sucrose by adding an equal amount of 80% sucrose. A gradient was formed by successive addition of 0.2 ml of 80% sucrose stock to the bottom of a polyallomer tube (13 by 51 mm), followed by 0.5 ml of 60% sucrose, 1.5 ml of 40% sucrose (containing the cell lysate), 0.8 ml of 35% sucrose, and 0.5-ml aliquots of 30, 25, 20, and 15% sucrose.

Sucrose solutions were prepared by mixing the appropriate amount of the gradient buffer (25 mM Tris-HCl [pH 7.5], 125 mM NaCl, 2 mM EDTA) and 80% sucrose. Tubes were centrifuged at 210,000 × g for 4 h at 4°C using an SW55 Ti rotor (Beckman Instruments). Gradients were fractionated into 0.2-ml aliquots withdrawn from the top of the tube, and radioactivity in each fraction was determined. The exact sucrose concentration in each fraction was determined with an Abbe refractometer. Fractions 1 to 10 (15 to 30% sucrose) contained detergent-insoluble lipid rafts.

For analysis of association of FcεRI with lipid rafts from γwt and γT52A RBL cells, the cells (15 × 10^6) were sensitized with ^{125}I-labeled DNP-specific IgE and activated or not with DNP-human serum albumin (HSA) conjugate (Sigma). Cells were lysed on ice in 1.0 ml of lysis buffer (0.1% Triton X-100, 20 mM Tris-HCl [pH 8.0], 140 mM NaCl, 2 mM EDTA, 1 mM Na$_3$VO$_4$, 1 mM PMSF, 0.5 U of aprotinin and 0.5 U of leupeptin per ml) as above. The gradient was formed by addition of 1 ml of 80% sucrose on the bottom of the tube followed by 2 ml of 40% sucrose containing the cell lysate and successive addition of 6 ml of 30% and 2.5 ml of 5% sucrose, and then centrifuged for 12 h at 200,000 × g in an L8-70 Beckman centrifuge. Eleven fractions were collected from the top of the gradient.

Cell activation, immunoprecipitation, immunoblotting, and kinase assay. Transfected cells were sensitized with TNP-specific IgE in suspension. After incubation for 30 min at 37°C, the cells were washed twice in BSS/BSA and activated for 5 min with TNP-BSA at a final concentration of 0.5 μg/ml. Towards the end of the activation period, the cells were briefly centrifuged and the pellet was resuspended in ice-cold 0.5 % Triton X-100 lysis buffer. After 20 min on ice, the lysate was centrifuged at 12,000 × g for 10 min to remove nuclei and insoluble remnants. IgE-FcεRI complexes, Syk, or LAT was immunoprecipitated from samples equivalent to 10^7 cells with rabbit anti-IgE, anti-Syk, or anti-LAT bound to UltraLink-immobilized protein A (Pierce), and immunoblotting with the corresponding antibodies was performed as described (2). Kinase activity of all Lyn-GFP constructs was determined by in vitro kinase assay as described (3).

Intracellular calcium measurements. Changes in the concentration of free intracellular Ca^{2+} ([Ca^{2+}]$_i$) in transfected cells expressing GFP or GFP-containing constructs were monitored using Fura Red AM probe (Molecular Probes). GFP and Fura Red have similar excitation but different emission maxima, allowing determination of [Ca^{2+}]$_i$ only in the transfected GFP-expressing cells. The transfected cells were sensitised with IgE and at 3 h postinfection were washed and loaded with Fura Red AM (4 μg/2 × 10^6 cells). After incubation for 1 h at 37°C, the cells were washed twice in PBS and transferred to tubes for flow cytometry. TNP-BSA at a final concentration of 0.5 μg/ml was added 60 s after the start of fluorescence-activated cell sorting (FACS) analysis, and thapsigargin (Sigma; 1 μM final concentration) was added at 180 s. The measurements were performed with a FACScan flow cytometer (Becton Dickinson) equipped with a single 488-nm argon laser used as the excitation source. GFP fluorescence was collected at 515 to 535 nm, and Fura Red emission at 665 to 685 nm using linear amplification. GFP-negative cells were gated out, and Fura Red fluorescence was collected at the indicated time intervals.

RESULTS

N-terminal myristoylation but not palmitoylation is required for Lyn kinase anchoring to the plasma membrane. The unique domain of Lyn kinase contains specific sequences for myristoylation and palmitoylation at positions Gly2 and Cys3, respectively. It has been shown that a mutation in the acylation sites of other members of the Src kinase family, Lck and Fyn, leads to their inability to associate with the plasma membrane (7, 39). To analyze the significance of N-terminal acylation and SH1 and SH2/SH3 domains for the anchoring of Lyn to the plasma membrane and partitioning in lipid rafts and the in vivo functional consequences thereof, we prepared various Lyn constructs with defects in one or both acylation sites as well as in SH domains. In all constructs GFP was added at the C terminus to allow fluorescence visualization of the constructs and to distinguish them from endogenous Lyn. The kinase activities of all constructs are shown in Fig. 1. The constructs were transfected into RBL cells using an SFV expression system, and the subcellular distribution of the constructs was analyzed at 4 h postinfection.

Confocal microscopy indicated that the constructs differed in their ability to associate with the nucleus and plasma membrane. As shown in Fig. 2A, GFP alone was evenly distributed throughout the cell and was included in the nucleus. It was not associated with the plasma membrane, as indicated by the absence of fluorescence overlap (yellow) with FcεRI. LynA-UNI and LynB-UNI were also found in the nucleus (not shown), whereas all other constructs were excluded from the nucleus. Wild-type LynB was mainly found associated with the plasma membrane, similar to the distribution of endogenous Lyn, as determined by biochemical means or indirect immunofluorescence of detergent-permeabilized cells (12, 15), demonstrating that the GFP tag did not affect the distribution of the transfected Lyn. It should also be noted that both GFP-tagged Lyn (Fig. 2A) and endogenous Lyn (12) accumulated in the perinuclear region. LynB-CA also localized to the plasma membrane, but LynB-GCA was found predominantly in the cytoplasm (Fig. 2A). Similar results were obtained when various Lyn constructs were analyzed in transfected BMMC and BMMC-Lyn$^{-/-}$ (not shown).

In order to verify the results of confocal microscopy, we analyzed the distribution of Lyn constructs by immunoblotting. As can be seen in Fig. 2B, endogenous Lyn was detectable as a double band of 53 and 56 kDa. Wild-type Lyn constructs (LynA-WT and LynB-WT), as well as a palmitoylation site mutant (LynB-CA) and the catalytically inactive Lyn (LynB-CI) were detected as bands of approximately 75 kDa. As expected, the myristoylation site-mutated Lyn (LynB-GA) and Lyn with mutations in both acylation sites (LynB-GCA) were not found in the plasma membrane fractions. LynA-SH2 (~55 kDa) as well as LynA-UNI (~40 kDa) and LynB-UNI (~35 kDa) were also associated with the plasma membrane, as detected by immunoblotting with anti-GFP antibody. Thus, association of Lyn with the plasma membrane is dependent on myristoylation of the N-terminal Gly in the unique domain, while other domains have no significant role in this anchoring.

It has been suggested that the Lyn localized in lipid rafts plays an important role in the phosphorylation of FcεRI and subsequent events (15, 16, 20, 38). To test this postulate, we first examined whether various Lyn constructs differed in their localization in lipid rafts. The data presented in Fig. 2C indicate that all Lyn constructs found in the plasma membrane fractions (see Fig. 2B) also partitioned to lipid rafts, with the exception of the palmitoylation-mutated Lyn (LynB-CA).
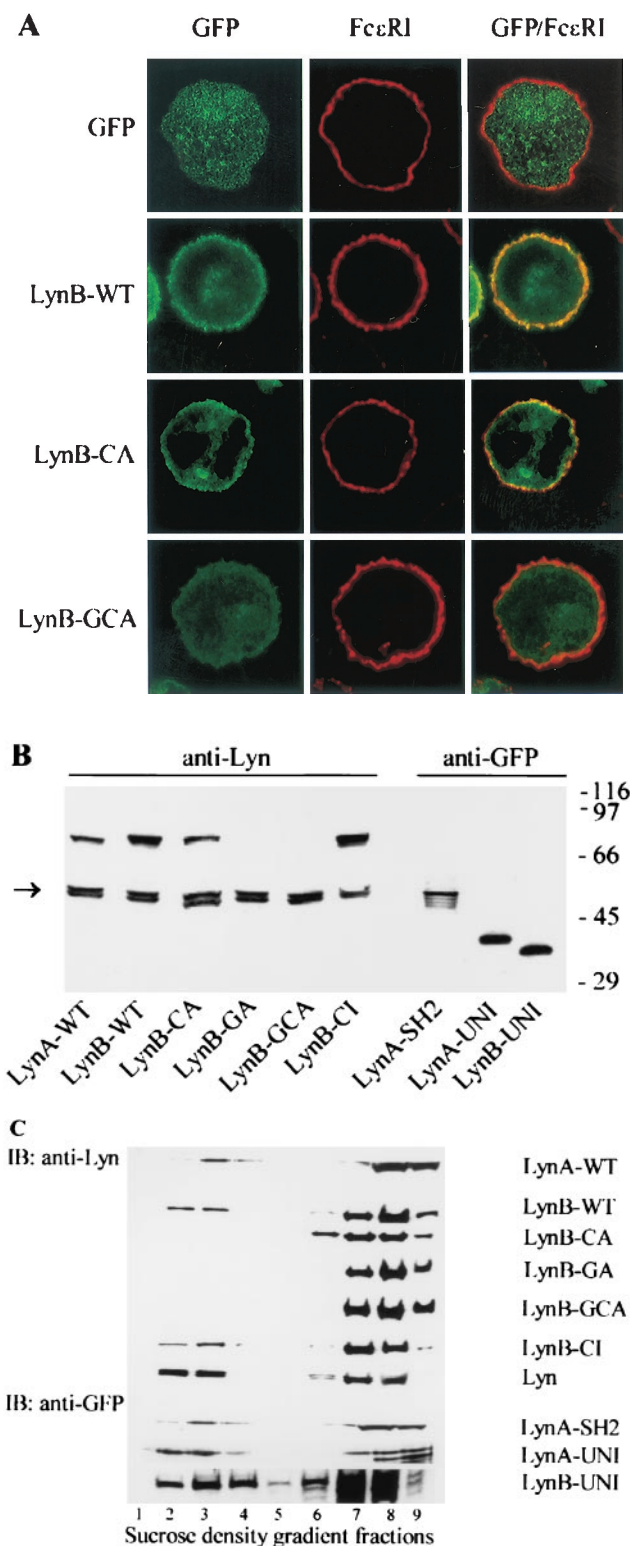
FIG. 2. Subcellular localization of different Lyn constructs. The indicated Lyn constructs were introduced into RBL cells. (A) Confocal images. Cells expressing GFP alone, wild-type LynB (LynB-WT), the Lyn palmitoylation site mutant (LynB-CA) or the Lyn myristoylation and palmitoylation site mutant (LynB-GCA) were fixed and stained for surface FcεRI using biotinylated IgE and Cy3-streptavidin. The left column shows the green fluorescence of Lyn-GFP constructs or GFP alone, the middle column shows the red fluorescence indicating FcεRI,

These results were obtained after solubilization of the transfected cells with 1% Triton X-100. Because previous studies indicated that association of aggregated FcεRI with lipid rafts is sensitive to Triton X-100 concentration (15, 16), we further analyzed the solubility of Lyn-CA at a lower concentrations of this detergent.

Using LynB-CA-transfected cells, we first confirmed that association of aggregated FcεRI with lipid raft fractions was dramatically decreased with increasing concentrations of Triton X-100. The result of a typical experiment is shown in Fig. 3. When the cells were solubilized with 0.06, 0.1, or 0.2% Triton X-100, $65.6\% \pm 2.4\%$, $52.9\% \pm 2.5\%$, and $15.2\% \pm 1.3\%$ of aggregated FcεRI was associated with lipid raft fractions, respectively (means $\pm$ standard deviation [SD] from three independent experiments in each group). It should be noted, however, that a significant amount ($7.9\% \pm 1.5\%$) of nonaggregated FcεRI was found in lipid raft fractions when 0.06% Triton was used.

Quantitative immunoblotting analysis indicated that in non-activated cells, lysed in 0.06% Triton, $5.3\% \pm 1.0\%$ of the LynB-CA construct was associated with lipid rafts (Table 1). Under these conditions, $31.1\% \pm 2.7\%$ of the transfected LynA-WT and $54.9\% \pm 5.9\%$ of the endogenous Lyn were found in lipid raft fractions. An increase to 0.1 and 0.2% Triton X-100 completely removed all LynB-CA from lipid raft fractions, whereas the amounts of the transfected LynA-WT and the endogenous Lyn were only slightly reduced. As expected, LynB-GCA, which is not anchored to the plasma membrane, was not found in lipid raft fractions under these conditions. We also analyzed the distribution of Src kinase, which, like LynB-CA, has only one acylation site and is not considered to be functionally associated with lipid rafts unless it is palmitoylated (39). Src kinase was found in light-density fractions after solubilization of the cells in 0.06 and 0.1% but not 0.2% Triton X-100. Thus, association of both Lyn-CA and Src with lipid raft fractions is extremely sensitive to low Triton X-100 concentrations.

To determine whether there are any changes in association of LynB-CA with lipid rafts after FcεRI aggregation, we performed another set of experiments in which surface FcεRI was aggregated by IgE–anti-IgE complexes and the amount of Lyn in lipid raft fractions was determined after solubilization of the cells in 0.06% Triton X-100, followed by sucrose density gradient fractionation and immunoblotting. Densitometric analysis indicated that FcεRI aggregation resulted in an increase in

and the right column shows the fluorescence overlap of merged images (in yellow). (B) Association of Lyn constructs with isolated membrane fractions. Membranes were isolated from RBL cells transfected with the indicated Lyn constructs, solubilized in 1% Triton X-100 lysis buffer, and size fractionated by SDS-PAGE. Lyn constructs were detected by immunoblotting with anti-Lyn (left) or anti-GFP (right) Abs. The left arrow indicates the position of endogenous p53/p56 Lyn. The positions of size markers (in kilodaltons) are shown on the right. (C) Association of Lyn constructs with lipid rafts. The cells were lysed in 1% Triton X-100 lysis buffer, and the whole lysates were fractionated by sucrose density gradient ultracentrifugation. Individual fractions, as indicated at the bottom, were analyzed for the presence of the indicated Lyn constructs or endogenous Lyn by immunoblotting (IB) as in panel B. Lipid rafts are present in fractions 2 to 4.
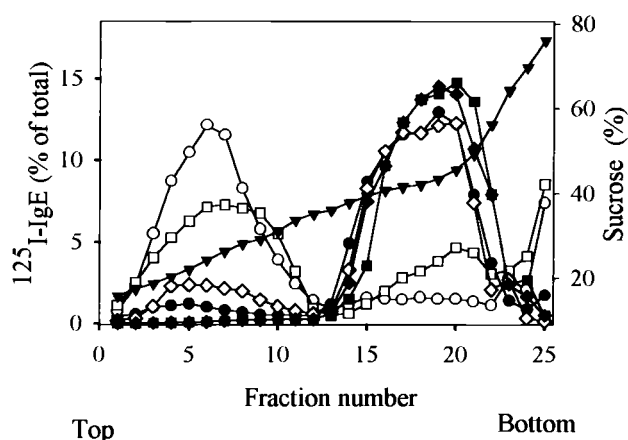
FIG. 3. Detergent-sensitive association of aggregated and unaggregated FcεRI with lipid rafts as detected by sucrose gradient analysis. RBL-2H3 cells were sensitized with [^{125}I]IgE (1 μg/ml), and [^{125}I]IgE-FcεRI complexes were aggregated (open symbols) or not (solid symbols) with rabbit anti-IgE antibody (10 μg/ml) for 5 min. The cells were solubilized on ice in a lysis buffer containing 0.06% (circles), 0.1% (squares), or 0.2% (diamonds) Triton X-100. Total cell lysates were loaded within 40% sucrose fractions of the sucrose step gradient and fractionated by ultracentrifugation for 4 h. Points show the percentage of total cpm present in individual fractions (left axis). The percentage of the FcεRI found in the lipid raft fractions was 65.6% ± 2.4%, 52.9% ± 2.5%, and 15.2% ± 1.3% for detergent concentrations of 0.06, 0.1, and 0.2%, respectively. Sucrose concentrations are also indicated (▼, right axis).

association of LynB-CA with lipid rafts from 5.3% ± 1.0% (see Table 1) to 10.3% ± 2.5% (three experiments). However, the significance of this increase is unclear, especially because under the same experimental conditions the fraction of LynB-WT in lipid rafts was similar in activated (28.9% ± 3.6%; three experiments) and resting cells (31.1% ± 2.7%; see Table 1).

Co-redistribution of Lyn kinase with aggregated FcεRI is dependent on Lyn N-terminal acylation, kinase activity, and conformation. FcεRI and fully acylated Lyn are uniformly distributed in the plasma membrane (Fig. 2A). If the FcεRI is aggregated with IgE and multivalent Ag or by other means, the complexes redistribute into small patches. As can be seen in the representative images in Fig. 4A, the aggregation of surface FcεRI in RBL cells results in co-redistribution of wild-type Lyn kinase (LynB-WT), as reflected by the formation of yellow patches from the overlay of green and red fluorescence profiles. An even more extensive co-redistribution was observed when Lyn with a deleted SH1 domain (LynA-SH2) was tested. The palmitoylation-defective Lyn construct (LynB-CA) showed decreased co-redistribution, indicating that a firm anchor into lipid rafts contributes to this process. GFP alone did not show any co-redistribution.

Quantitative analysis of co-redistribution of various Lyn constructs with aggregated FcεRI in RBL cells is shown in Fig. 4B. To determine the role of endogenous Lyn in the co-redistribution of the transfected Lyn constructs with aggregated FcεRI, we also used wild-type BMMC and BMMC-Lyn$^{-/-}$. The wild-type Lyn showed a co-redistribution which was similar in all three cell lines used. Palmitoylation-defective Lyn exhibited a decreased co-redistribution which was not dependent on endogenous Lyn, as reflected by the same extent of

co-redistribution in BMMC and BMMC-Lyn$^{-/-}$. A defect in both acylation sites (LynB-GCA) and, therefore, the absence of anchoring in the plasma membrane resulted in the absence of co-redistribution.

Interestingly, the absence of co-redistribution was also observed in LynA-UNI (Fig. 4B) and LynB-UNI (not shown), indicating that anchoring to the plasma membrane and lipid rafts is not sufficient for the co-redistribution and that possibly the kinase activity and SH2/SH3 domains play a significant role. This assumption was confirmed by examination of the properties of Lyn with a mutation in the catalytic domain (LynB-CI). This construct exhibited co-redistribution with aggregated FcεRI comparable to the wild-type Lyn in RBL cells and BMMC. However, when LynB-CI was transfected into BMMC-Lyn$^{-/-}$, no co-redistribution of LynB-CI with aggregated FcεRI was observed, indicating that the endogenous Lyn activity was necessary to mediate the co-redistribution. Additionally, the highest level of co-redistribution was observed when the LynA-SH2 construct was used. In RBL cells and BMMC, the cross-correlation coefficients attained were 0.78 ± 0.07 and 0.81 ± 0.07, respectively. However, in the absence of endogenous Lyn (BMMC-Lyn$^{-/-}$), the co-redistribution of LynA-SH2 dropped to 0.31 ± 0.09.

Palmitoylation-defective Lyn kinase is able to initiate early stages of FcεRI-mediated activation. To find out whether or not Lyn kinase must be anchored in the plasma membrane and lipid rafts to initiate early FcεRI-mediated activation events, we transfected various Lyn constructs into BMMC-Lyn$^{-/-}$ and followed the tyrosine phosphorylation of FcεRIβ and γ subunits, Syk kinase, and the LAT adaptor. For these experiments, we used constructs with Lyn kinase activity, namely, LynB-WT, palmitoylation-deficient LynB-CA, and myristoylation- and palmitoylation-deficient Lyn-B-GCA. In all experiments, a construct with GFP alone served as the negative control. The transfected cells were sensitized with IgE and stimulated with TNP-BSA. Five minutes later the cells were lysed, and FcεRI, Syk, or LAT was precipitated using the appropriate Abs. The immunoprecipitates were size fractionated by sodium dodecyl sulfate-polyacrylamide gel electrophoresis (SDS-PAGE) and analyzed by immunoblotting.

TABLE 1. Quantitative immunoblotting analysis of various Lyn constructs and endogenous Lyn and Src kinase in lipid raft fractions after solubilization of transfected RBL cells with different concentrations of Triton X-100[a]

Kinase analyzed	Mean % of kinase in lipid raft fraction ± SD (no. of expt) at Triton X-100 concn:		
	0.06%	0.1%	0.2%
Transfected kinase			
LynA-WT	31.1 ± 2.7 (3)	30.4 ± 3.2 (3)	28.2 ± 4.0 (3)
LynB-CA	5.3 ± 1.0 (4)	0.0 ± 0.0 (2)	0.0 ± 0.0 (2)
LynB-GCA	0.0 ± 0.0 (2)	NT	NT
Endogenous kinase			
Lyn	54.9 ± 5.9 (7)	51.2 ± 1.9 (3)	47.2 ± 5.2 (3)
Src	18.8 ± 3.3 (4)	14.4 ± 2.0 (3)	0.0 ± 0.0 (2)

[a] Values indicate means ± SD of the percentage of kinases in lipid raft fractions (15 to 30% sucrose) after solubilization of the cells in the indicated concentrations of Triton X-100 and fractionation on sucrose density gradients. Numbers in parentheses indicate number of independent experiments performed. NT, not tested.
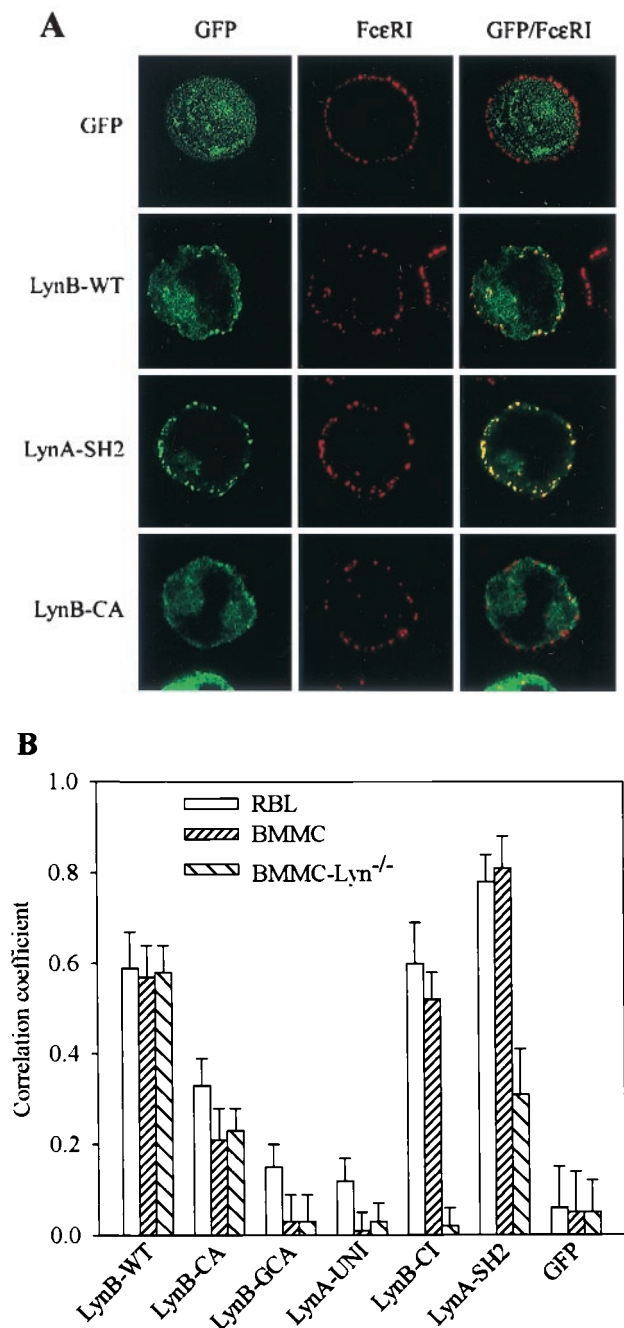
FIG. 4. Co-redistribution of Lyn constructs with aggregated FcεRI. The indicated Lyn constructs or GFP alone was introduced into RBL cells, BMMC, or BMMC-Lyn⁻/⁻. Cells were sensitized with biotinylated IgE, and surface FcεRI-IgE complexes were aggregated with Cy3-conjugated streptavidin for 2 min. The cells were fixed and analyzed by confocal microscopy. (A) Confocal images of RBL cells. Images are arranged as in Fig. 2A. (B) Quantitative analysis of co-redistribution of the indicated Lyn constructs with aggregated FcεRI in RBL cells, BMMC, and BMMC-Lyn⁻/⁻. Means ± SD of correlation coefficients were calculated from at least two independent experiments, with 12 to 16 cells analyzed in each experiment.

Representative data in Fig. 5A from three experiments indicate that following the FcεRI engagement, both the LynB-WT and LynB-CA transfectants exhibited an increased tyrosine phosphorylation of FcεRI β and γ subunits and an asso-

ciated protein of about 70 kDa. In contrast, the engagement of FcεRI in cells transfected with LynB-GCA or GFP alone did not result in increased tyrosine phosphorylation of FcεRI subunits and the associated 70-kDa protein. The absence of the signal was not due to the absence of the receptor in immunoprecipitated material, as indicated by the results of immunoblotting with an MAb specific for the FcεRI-β subunit.

Similar results were obtained when Syk and LAT immunoprecipitates were analyzed. Thus, the engagement of FcεRI resulted in increased Syk and LAT tyrosine phosphorylation in cells transfected with LynB-WT and LynB-CA (Fig. 5B and C). Quantitative analysis of the immunoblots, which took into account the infection efficiencies, indicated that the level of FcεRI, Syk, and LAT tyrosine phosphorylation increased to a similar extent in LynB-WT and LynB-CA cells (Fig. 5D). No increase in Syk and LAT tyrosine phosphorylation was observed in activated cells with the GFP construct. It should be noted that in LynB-GCA-transfected cells, some increase in tyrosine phosphorylation of Syk and LAT was observed. This was apparently due to the Lyn kinase activity of the LynB-GCA construct.

An increase in $[Ca^{2+}]_i$ is one of the early signs of cell activation. In further experiments we measured $[Ca^{2+}]_i$ in BMMC-Lyn⁻/⁻ transfected with various constructs following activation via FcεRI (Fig. 6A). For these measurements, the cells were loaded with Fura Red AM, a specific indicator of free Ca^{2+}, and $[Ca^{2+}]_i$ was only determined in transfected cells, i.e., those expressing GFP. As seen in Fig. 6B, cells transfected with wild-type Lyn (LynB-WT) showed a significant increase in $[Ca^{2+}]_i$ after FcεRI engagement, 49% ± 6% of the maximum increase in $[Ca^{2+}]_i$ observed in cells exposed to thapsigargin. In cells transfected with the palmitoylation-deficient LynB-CA, the FcεRI engagement also resulted in a significant increase in $[Ca^{2+}]_i$. However, this increase was slightly lower (41% ± 7%) and reached its maximum with some delay. FcεRI engagement in cells expressing the myristoylation- and palmitoylation-deficient LynB-GCA induced only a small increase in $[Ca^{2+}]_i$ (15% ± 3% of maximal release) that was comparable to that in negative controls transfected with GFP alone (10% ± 4%).

Is constitutively phosphorylated FcεRI associated with lipid rafts? In the experiments described above, we showed that LynB-CA is able to phosphorylate FcεRI and trigger early signaling events. Because LynB-CA seems to be excluded from lipid rafts, at least those defined by resistance to ≥0.1% Triton X-100, the above data suggested that FcεRI could be phosphorylated outside the lipid rafts. To further analyze this possibility, we studied the lipid raft association of a constitutively tyrosine-phosphorylated FcεRI that results from the expression of a mutant γ chain (Thr52 to Ala) in RBL-2H3-γ⁻ cells (45). This mutation, resulting in constitutive tyrosine phosphorylation of FcεRI, could cause a conformational change of FcεRIγ, allowing its tyrosine phosphorylation *cis*- or *trans*-molecularly. Alternatively, the T52A mutation could cause the constitutive formation of FcεRI aggregates that would then be targeted to lipid rafts, where they would become phosphorylated. In this case, an increased amount of FcεRIγT52A should be detected in lipid rafts.

First, we wanted to confirm, using a slightly different experimental setup, that FcεRI from γT52A is constitutively tyrosine phosphorylated. Tyrosine phosphorylation of FcεRIγ was an-
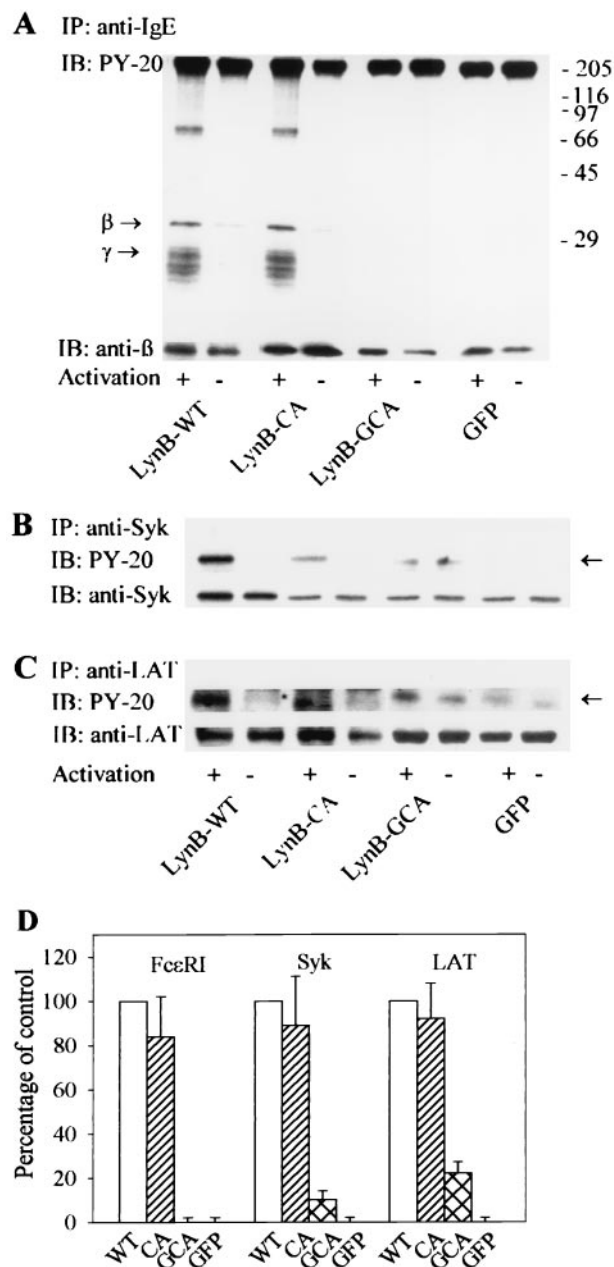
FIG. 5. Antigen-induced tyrosine phosphorylation of FcεRI, Syk, and LAT in cells expressing palmitoylation site-mutated Lyn. BMMC-Lyn$^{-/-}$ were transfected with LynB-WT, LynB-CA, LynB-GCA, or GFP alone. The transfected and IgE-sensitized cells were activated or not with TNP-BSA for 5 min. The cells were lysed, and FcεRI complexes, Syk, or LAT was immunoprecipitated from the postnuclear supernatants using Abs specific for IgE (A), Syk (B), or LAT (C). Proteins were resolved by SDS-PAGE and analyzed by immunoblotting (IB) with antiphosphotyrosine MAb PY-20-HRP. After stripping, MAbs specific for FcεRI β subunit, Syk, and LAT were used to estimate the relative amounts of the immunoprecipitated (IP) protein. Arrows indicate the positions of the phosphorylated β and γ subunits of the FcεRI (A), Syk (B), and LAT (C). (A) Positions of size markers are shown on the right (in kilodaltons). (D) Quantitative analysis of tyrosine phosphorylation of immunoprecipitated FcεRI, Syk, and LAT from cells transfected with LynB-WT (WT), LynB-CA (CA), LynB-GCA (GCA), or GFP alone. Tyrosine phosphorylation of FcεRI, Syk and LAT from cells transfected with LynB-WT was taken as 100%. Means ± SD were calculated from four independent experiments in each group. Data were normalized for different transfections efficiencies as determined by flow cytofluorometry.
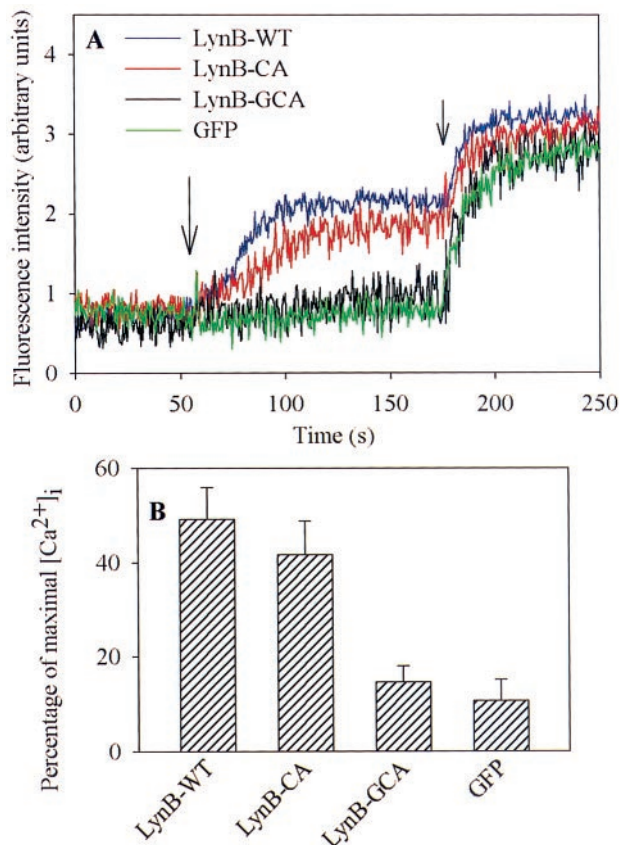

FIG. 6. Antigen-induced increase in $[Ca^{2+}]_i$ in cells expressing palmitoylation site-mutated Lyn. (A) BMMC-Lyn$^{-/-}$ were transfected with LynB-WT, LynB-CA, LynB-GCA, or GFP alone. The cells were sensitized with IgE and loaded with Fura Red AM. At 3 h postinfection, the cells were stimulated with TNP-BSA, and $[Ca^{2+}]_i$ was determined only in transfected cells by double-color FACS analysis. The inverse of the quenching of Fura Red fluorescence intensity (rise in intracellular calcium) in transfected cells is reported as a function of time. The long arrow and short arrow indicate time of addition of the antigen and thapsigargin, respectively. (B) The extent of activation is expressed as a ratio between the decrease in Fura Red fluorescence in FcεRI-activated cells and that observed after addition of thapsigargin, which was taken as 100%. Means ± SD were calculated from six to eight experiments in each group.

alyzed by immunoprecipitation of tyrosine-phosphorylated proteins with 4G10 antibody followed by immunoblotting with an antibody to FcεRIγ. The data presented in Fig. 7 indicate that FcεRIγ from resting γT52A cells exhibits tyrosine phosphorylation similar to that of FcεRIγ from antigen-activated γwt cells. Antigen aggregation of FcεRIγT52A led to a further increase in its tyrosine phosphorylation, which correlated with its inclusion in lipid rafts (see below). The observed differences in FcεRIγ tyrosine phosphorylation were not due to different amounts of proteins immunoprecipitated, as indicated by the same amount of Shc, which is tyrosine phosphorylated in both resting and activated cells exposed to serum (47).

The fraction of FcεRI in lipid rafts was measured as the percentage of radioactivity in the light-density fractions (fractions 2 to 5; 5 to 30% sucrose) after solubilization of ^{125}I-sensitized cells in 0.1% Triton X-100 and fractionation on sucrose density gradient. When γwt cells were used, only a
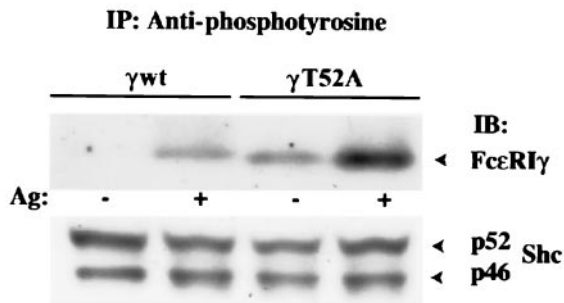
IP: Anti-phosphotyrosine

FIG. 7. Tyrosine phosphorylation of FcεRI from γwt and γT52A cells. The cells (5×10^6) were sensitized with IgE and stimulated (+) or not (−) with 0.1 μg of DNP-HSA (Ag). After 5 min the cells were lysed in 1% Triton X-100-containing lysis buffer, and tyrosine-phosphorylated proteins were immunoprecipitated (IP) with MAb 4G10. Immunoblots (IB) were probed with chicken antibody to FcεRIγ, followed by stripping and sequential immunoblotting with an antibody recognizing constitutively phosphorylated p46 and p52 isoforms of Shc as a loading control.

small fraction of FcεRI ($4.0\% \pm 0.7\%$; three experiments) was associated with light-density fractions. Under the same experimental conditions, a similar amount of FcεRI from γT52A was found in lipid raft fractions ($3.9\% \pm 0.6\%$). After antigen-mediated aggregation, a significant increase in the amount of γwt-derived FcεRI in lipid raft fractions was observed ($41.9\% \pm 5.0\%$), but again similar values where attained when FcεRI from γT52A was analyzed ($43.1\% \pm 4.1\%$). These data indicate that constitutive tyrosine phosphorylation of FcεRIγT52A is not due to its higher association with lipid rafts and support the notion that it can be phosphorylated outside lipid rafts.

DISCUSSION

The results presented in this study show that Lyn kinase must be anchored in the plasma membrane, but not necessarily firmly in lipid rafts, to be able to initiate early stages of cell activation mediated by FcεRI. The first step in this process is aggregation of the FcεRI by multivalent ligand and subsequent tyrosine phosphorylation of its β and γ subunits by Lyn kinase (14, 31). This is followed by tyrosine phosphorylation of other signaling molecules (see the introduction). Interestingly, most of these molecules have been shown to transiently co-redistribute with the aggregated FcεRI (5, 42). As shown in this study, as well as in a previous report (20), Lyn exhibits a homogenous distribution on the plasma membrane before activation, as detected by fluorescence microsocopy, and moves after FcεRI aggregation into regions of aggregated FcεRI. Quantitative analysis revealed that the co-redistribution of Lyn and aggregated FcεRI depends on several structural and functional properties of the Lyn kinase.

First, Lyn must be fatty acylated in the N-terminal end of the molecule. In the absence of both palmitoylation and myristoylation, no anchoring of Lyn into the plasma membrane is observed and there is no co-redistribution of Lyn with aggregated FcεRI. The absence of membrane anchoring and co-redistribution with FcεRI was found not only in the Lyn-GCA construct, with both acylation sites mutated, but also in the Lyn-GA construct, with a mutation in the myristoylation site.

This is consistent with previous data indicating that N-myristoylation is a necessary prerequisite for palmitoylation (7). The absence of palmitoylation in the LynB-CA mutant resulted in its decreased ability to localize into lipid rafts but did not preclude its association with the plasma membrane. The LynB-CA mutant exhibited a decreased co-redistribution with aggregated FcεRI. This inhibition was similar in RBL, BMMC, and BMMC-Lyn$^{-/-}$, indicating that it is independent of the presence of the endogenous Lyn. Importantly, the decreased ability to associate with lipid rafts and the decreased co-redistribution with aggregated FcεRI did not interfere with the ability of the Lyn-CA mutant to initiate early FcεRI phosphorylation and activation of early events (see below).

Second, the inhibition of kinase activity caused by mutating Lys279 to Arg in full-length Lyn B kinase (LynB-CI) had no effect on anchoring of this mutant kinase to the plasma membrane and lipid rafts, but completely suppressed its co-redistribution with aggregated FcεRI. This suppression was observed after transfection of LynB-CI into BMMC-Lyn$^{-/-}$ but not into BMMC and RBL cells, which express an endogenous Lyn. These data, together with the comparable co-redistribution of wild-type Lyn with aggregated FcεRI in both BMMC and BMMC-Lyn$^{-/-}$, indicated that Lyn kinase activity in *cis* or *trans* was necessary for proper Lyn-FcεRI interaction.

Third, consistent with these data, the removal of the catalytic domain in the LynA-SH2 construct had no effect on Lyn's incorporation in the plasma membrane and lipid rafts but inhibited co-redistribution of this construct with aggregated FcεRI in BMMC-Lyn$^{-/-}$. Compared to LynB-CI, the extent of inhibition was smaller, suggesting that the absence of the kinase domain and/or the regulatory C-terminal tyrosine induced a conformational change improving its co-redistribution. In accord with this interpretation, LynA-SH2, exhibited a higher degree of co-redistribution with FcεRI in RBL and BMMC than wild-type Lyn.

Fourth, LynA-UNI and LynB-UNI, which lack the SH1, SH2, and SH3 domains but retain both acylation sites, localized properly in the plasma membrane and in lipid rafts but failed to show any co-redistribution with aggregated FcεRI. The absence of recruitment of the Lyn unique domains into regions of aggregated FcεRI was observed after transfection of the Lyn constructs not only into BMMC-Lyn$^{-/-}$, but also into BMMC and RBL cells, i.e., cells expressing endogenous wild-type Lyn. These data, together with the finding of normal colocalization of LynB-CI in cells expressing endogenous Lyn (see above), suggest that the SH2 and SH3 domains are involved in the recruitment of Lyn to the phosphorylated receptors. Our findings are consistent with in vitro studies (25) demonstrating that the SH2 domain of Lyn interacts with the phosphorylated ITAM of the FcεRIβ subunit; consequently, we assume that this interaction is likely involved in the LynB-CI recruitment.

The relationship between patches of aggregated FcεRI, as determined by confocal microscopy, and lipid rafts with aggregated FcεRI, as determined by biochemical analysis of detergent-solubilized cells, is not completely clear and will require further study. However, our confocal microscopy findings that Lyn constructs exhibited different potentials to colocalize with patches of aggregated FcεRI and that this association corresponded to the activation potential of the constructs indicated

that association of Lyn and FcεRI in patches has a physiological significance. Furthermore, because most of the aggregated FcεRI was located in small patches on the cell surface and at the same time was found associated with lipid rafts, it is very likely that microscopic patches of aggregated FcεRI are found in lipid raft fractions of the sucrose gradient, especially when analysis is performed at early stages of receptor activation.

Thus, the collective data favor the co-redistribution of Lyn with FcεRI as reflecting an SH2 domain-dependent redistribution of Lyn that follows the initial phosphorylation of the FcεRI by a constitutive but weakly associated Lyn kinase. This view is supported by the requirement of Lyn kinase activity for co-redistribution of Lyn-CI in the BMMC-Lyn$^{-/-}$ by the enhanced co-redistribution of a Lyn-SH2 construct, and by our inability to observe the previously described weak interaction of Lyn-UNI with FcεRI (48) in the co-redistribution assay. Regardless, the confocal studies demonstrated the unique failure of the SH2 domain-containing and catalytically active Lyn-CA to co-redistribute with the FcεRI in the presence or absence of endogenous Lyn. As this Lyn construct is not effectively recruited to lipid rafts (based on our biochemical data), our findings argue the importance of Lyn residence in lipid rafts for the SH2-dependent redistribution of Lyn with FcεRI and suggest that this takes place in lipid rafts.

The most important finding of this work is the evidence that LynB-CA, unlike LynB-GCA, was able to initiate early stages of mast cell activation, including tyrosine phosphorylation of FcεRI β and γ subunits, Syk kinase, and LAT and an increase in $[Ca^{2+}]_i$. These data support the concept that Lyn kinase anchored to the plasma membrane but not necessarily to lipid rafts (defined by resistance to detergents) is important for early stages of mast cell activation. Thus, our data are more consistent with the model suggesting that Lyn kinase in resting cells is somehow weakly associated with a small fraction of FcεRI. This association requires Lyn myristoylation and its anchoring into the plasma membrane. The initial phosphorylation of the receptor subunits but not their extensive aggregation promotes a transient association of more Lyn, thereby shifting the balance between phosphorylation and dephosphorylation state (see protein-protein model in the introduction).

Several recent findings support this notion. Using a yeast two-hybrid system, direct interaction was detected between Lyn or its unique domain and the C-terminal cytoplasmic domain of the FcεRI β subunit (48). Next, immunoelectron microscopic studies of nonactivated cells indicated that FcεRI and Lyn are localized in the plasma membrane in small clusters and that approximately 25% of the FcεRI clusters contained Lyn (50). Furthermore, functional studies indicated that catalytically active or inactive Lyn chimeric constructs, which did not localize in lipid rafts, were able to potentiate or inhibit, respectively, aggregation-induced phosphorylation of receptors (49). Finally, our data indicating that constitutively tyrosine-phosphorylated FcεRI from resting γT52A cells and unphosphorylated FcεRI from resting γwt cells exhibit the same density on sucrose gradients suggest that FcεRI can be tyrosine phosphorylated in the absence of aggregation and increased association with lipid rafts.

Although our data indicate that Lyn must be anchored in the plasma membrane for its proper signaling, they do not support the model suggesting that Lyn kinase sequestered in lipid rafts

is necessary for FcεRI-induced phosphorylation (see the introduction). That concept was inferred from observations that the aggregated and tyrosine-phosphorylated FcεRI, derived from nonionic-detergent-solubilized activated cells, was found in the buoyant fraction of lipid rafts, together with Lyn kinase and glycosyl phosphatidylinositol (GPI)-anchored proteins (15–17). Furthermore, cholesterol depletion induced by a 60-min incubation of RBL cells with 10 mM methyl-β-cyclodextrin inhibited the co-redistribution of Lyn with aggregated FcεRI, association of aggregated FcεRI with lipid rafts, and tyrosine phosphorylation of the FcεRI subunits (20, 38). However, newer data indicate that a shorter treatment of RBL cells with 10 mM methyl-β-cyclodextrin, which removed approximately 60% of cholesterol and led to almost complete solubilization of Lyn kinase in Triton X-100 with only a negligible effect on tyrosine phosphorylation of Syk kinase, could dramatically potentiate the FcεRI-mediated secretory response (44).

However, it should be noted that all studies to date, including the present one, do not rule out a role for lipid rafts in FcεRI signaling. In fact, we observed an additional increase in phosphorylation of the constitutively tyrosine-phosphorylated FcεRIγT52A upon antigen aggregation, an event which enhanced its association with lipid rafts. This suggests the possibility that Lyn in lipid rafts may function to sustain the activation state of the FcεRI in an SH2 domain-dependent manner. Nevertheless, we also observed the normal phosphorylation of LAT, a lipid raft-resident protein (53), and normal calcium signals independent of Lyn residence in lipid rafts but dependent on Lyn anchoring to the plasma membrane. Thus, because we observed normal calcium signals and LAT is required for this event in mast cells (37), its phosphorylation in lipid rafts can occur independently of Lyn residence in lipid rafts.

Data seemingly contradictory to ours were obtained by Honda and coworkers, who found that only the palmitoylated Src kinases were able to physically interact with FcεRI and to mediate signal transduction (21). However, in their experiments the activity of endogenous Src family kinases was first suppressed by introduction of a membrane-anchored C-terminal Src kinase (m-Csk) and then reconstituted with Src family kinases whose C-terminal negative regulatory sequence was replaced with a c-Myc epitope. Thus, as the authors themselves admit, in this system one cannot exclude the possibility that the transfected Src kinases competed for the inhibitory activity of m-Csk and that FcεRI signaling was in fact initiated by the endogenous Src kinases instead of the transfected ones. Recent findings that a Csk binding protein, Cbp (24) or PAG (8), is associated with lipid rafts, and therefore only lipid raft-anchored kinases could compete with the substrate, make this scenario plausible.

Taken together, the combined data suggest that the constitutive and functional association between Lyn and FcεRI can occur outside the lipid rafts. Nevertheless, membrane lipids seem to be involved in the proper positioning of Lyn in the plasma membrane of both resting and activated cells. The formation of large receptor aggregates in the course of activation by multivalent antigen could lead to changes in lipids surrounding the FcεRI, and this could explain previous observations of a redistribution of some lipids in FcεRI-activated cells (20, 42). Lipids involved not just in anchoring Lyn in the

plasma membrane but also in co-localization of Lyn with FcεRI in resting cells could conceivably be responsible for the signaling capacity of FcεRI or of chimeras lacking the β subunit (1, 27), by stabilizing or promoting weak interactions with the γ cytoplasmic tail (34, 49).

ACKNOWLEDGMENTS

REFERENCES

1. Alber, G. L., L. Miller, C. L. Jelsema, N. Varin-Blank, and H. Metzger. 1991. Structure-function relationships in the mast cell high affinity receptor for IgE. J. Biol. Chem. 266:22613–22620.
2. Amoui, M., L. Dráberová, P. Tolar, and P. Dráber. 1997. Direct interaction of Syk and Lyn protein tyrosine kinases in rat basophilic leukemia cells activated via type I Fcε receptor. Eur. J. Immunol. 27:321–328.
3. Amoui, M., P. Dráber, and L. Dráberová. 1997. Src family-selective tyrosine kinase inhibitor, PP1, inhibits both FcεRI- and Thy-1-mediated activation of rat basophilic leukemia cells. Eur. J. Immunol. 27:1881–1886.
4. Arudchandran, R., M. J. Brown, J. S. Song, S. A. Wank, H. Haleem-Smith, and J. Rivera. 1999. Polyethylene glycol-mediated infection of non-permissive mammalian cells with Semliki Forest virus: application to signal transduction studies. J. Immunol. Methods 222:197–208.
5. Arudchandran, R., M. J. Brown, M. J. Peirce, J. S. Song, J. Zhang, R. P. Siraganian, U. Blank, and J. Rivera. 2000. The Src homology 2 domain of Vav is required for its compartmentation to the plasma membrane and activation of c-Jun NH₂-terminal kinase 1. J. Exp. Med. 191:47–59.
6. Benhamou, M., N. J. P. Ryba, H. Kihara, H. Nishikata, and R. P. Siraganian. 1993. Protein-tyrosine kinase p72^syk in high affinity IgE receptor signaling. J. Biol. Chem. 268:23318–233324.
7. Bijlmakers, M. J., M. Isobe-Nakamura, L. J. Ruddock, and M. Marsh. 1997. Intrinsic signals in the unique domain target p56^lck to the plasma membrane independently of CD4. J. Cell Biol. 137:1029–1040.
8. Brdička, T., D. Pavlištová, A. Leo, E. Bruyns, V. Kořínek, P. Angelisová, J. Scherer, A. Shevchenko, I. Hilgert, J. Černý, K. Drbal, Y. Kuramitsu, B. Kornacker, V. Hořejší, and B. Schraven. 2000. Phosphoprotein associated with glycosphingolipid-enriched microdomains (PAG), a novel ubiquitously expressed transmembrane adaptor protein, binds the protein tyrosine kinase csk and is involved in regulation of T cell activation. J. Exp. Med. 191:1591–1604.
9. Brown, D. A., and E. London. 1998. Functions of lipid rafts in biological membranes. Annu. Rev. Cell Dev. Biol. 14:111–136.
10. Cheng, P. C., M. L. Dykstra, R. N. Mitchell, and S. K. Pierce. 1999. A role for lipid rafts in B cell antigen receptor signaling and antigen targeting. J. Exp. Med. 190:1549–1560.
11. Dráberová, L., and P. Dráber. 1991. Functional expression of the endogenous Thy-1 gene and the transfected murine Thy-1.2 gene in rat basophilic leukemia cells. Eur. J. Immunol. 21:1583–1590.
12. Dráberová, L., E. Dráberová, Z. Surviladze, P. Dráber, and Pa. Dráber. 1999. Protein tyrosine kinase p53/p56^lyn forms complexes with γ-tubulin in rat basophilic leukemia cells. Int. Immunol. 11:1829–1839.
13. Dráberová, L., M. Amoui, and P. Dráber. 1996. Thy-1-mediated activation of rat mast cells: the role of Thy-1 membrane microdomains. Immunology 87:141–148.
14. Eiseman, E., and J. B. Bolen. 1992. Engagement of the high-affinity IgE receptor activates src protein-related tyrosine kinases. Nature 355:78–80.
15. Field, K. A., D. Holowka, and B. Baird. 1995. FcεRI-mediated recruitment of p53/56^lyn to detergent-resistant membrane domains accompanies cellular signaling. Proc. Natl. Acad. Sci. USA 92:9201–9205.
16. Field, K. A., D. Holowka, and B. Baird. 1997. Compartmentalized activation of the high affinity immunoglobulin E receptor within membrane domains. J. Biol. Chem. 272:4276–4280.
17. Field, K. A., D. Holowka, and B. Baird. 1999. Structural aspects of the association of FcεRI with detergent-resistant membranes. J. Biol. Chem. 274:1753–1758.
18. Haleem-Smith, H., E. Y. Chang, Z. Szallasi, P. M. Blumberg, and J. Rivera. 1995. Tyrosine phosphorylation of protein kinase C-δ in response to the activation of the high-affinity receptor for immunoglobulin E modifies its substrate recognition. Proc. Natl. Acad. Sci. USA 92:9112–9116.

19. Hibbs, M. L., D. M. Tarlinton, J. Armes, D. Grail, G. Hodgson, R. Maglitto, S. A. Stacker, and A. R. Dunn. 1995. Multiple defects in the immune system of Lyn-deficient mice, culminating in autoimmune disease. Cell 83:301–311.
20. Holowka, D., E. D. Sheets, and B. Baird. 2000. Interactions between FcεRI and lipid raft components are regulated by the actin cytoskeleton. J. Cell Sci. 113:1009–1019.
21. Honda, Z., T. Suzuki, H. Kono, M. Okada, T. Yamamoto, C. Ra, Y. Morita, and K. Yamamoto. 2000. Sequential requirements of the N-terminal palmitoylation site and SH2 domain of Src family kinases in the initiation and progression of FcεRI signaling. Mol. Cell. Biol. 20:1759–1771.
22. Hutchcroft, J. E., R. L. Geahlen, G. G. Deanin, and J. M. Oliver. 1992. FcεRI-mediated tyrosine phosphorylation and activation of the 72-kD protein-tyrosine kinase, PTK72, in RBL-2H3 rat tumor mast cells. Proc. Natl. Acad. Sci. USA 89:9107–9111.
23. Janes, P. W., S. C. Ley, and A. I. Magee. 1999. Aggregation of lipid rafts accompanies signaling via the T cell antigen receptor. J. Cell Biol. 147:447–461.
24. Kawabuchi, M., Y. Satomi, T. Takao, Y. Shimonishi, S. Nada, K. Nagai, A. Tarakhovsky, and M. Okada. 2000. Transmembrane phosphoprotein Cbp regulates the activities of Src-family tyrosine kinases. Nature 404:999–1003.
25. Kihara, H., and R. P. Siraganian. 1994. Src homology 2 domains of Syk and Lyn bind to tyrosine-phosphorylated subunit of the high affinity IgE receptor. J. Biol. Chem. 269:22427–22432.
26. Li, W., G. G. Deanin, B. Margolis, J. Schlessinger, and J. M. Oliver. 1992. FcεRI-mediated tyrosine phosphorylation of multiple proteins, including phospholipase Cγ1 and the receptor βγ2 complex, in RBL-2H3 rat basophilic leukemia cells. Mol. Cell. Biol. 12:3176–3182.
27. Lin, S., C. Cicala, A. M. Scharenberg, and J. P. Kinet. 1996. The FcεRIβ subunit functions as an amplifier of FcεRIγ-mediated cell activation signals. Cell 85:985–995.
28. Minoguchi, K., M. Benhamou, W. D. Swaim, Y. Kawakami, T. Kawakami, and R. P. Siraganian. 1994. Activation of protein tyrosine kinase p72^syk by FcεRI aggregation in rat basophilic leukemia cells. J. Biol. Chem. 269:16902–16908.
29. Montixi, C., C. Langlet, A. M. Bernard, J. Thimonier, C. Dubois, M. A. Wurbel, J. P. Chauvin, M. Pierres, and H. T. He. 1998. Engagement of T cell receptor triggers its recruitment to low-density detergent-insoluble membrane domains. EMBO J. 17:5334–5348.
30. Ortega, E., M. Lara, I. Lee, C. Santana, A. M. Martinez, J. R. Pfeiffer, R. J. Lee, B. S. Wilson, and J. M. Oliver. 1999. Lyn dissociation from phosphorylated FcεRI subunits: A new regulatory step in the FcεRI signaling cascade revealed by studies of FcεRI dimer signaling activity. J. Immunol. 162:176–185.
31. Paolini, R., M. H. Jouvin, and J. P. Kinet. 1991. Phosphorylation and dephosphorylation of the high-affinity receptor for immunoglobulin E immediately after receptor engagement and disengagement. Nature 353:855–858.
32. Perez-Montfort, R., J. P. Kinet, and H. Metzger. 1983. A previously unrecognized subunit of the receptor for immunoglobulin E. Biochemistry 22:5722–5728.
33. Pribluda, V. S., C. Pribluda, and H. Metzger. 1994. Transphosphorylation as the mechanism by which the high-affinity receptor for IgE is phosphorylated upon aggregation. Proc. Natl. Acad. Sci. USA 91:11246–11250.
34. Repetto, B., G. Bandara, J. Kado Fong, J. D. Larigan, G. A. Wiggan, D. Pocius, M. Basu, A. M. Gilfillan, and J. P. Kochan. 1996. Functional contributions of the FcεRIα and FcεRIγ subunit domains in FcεRI-mediated signaling in mast cells. J. Immunol. 156:4876–4883.
35. Rivera, J., J. P. Kinet, J. Kim, C. Pucillo, and H. Metzger. 1988. Studies with a monoclonal antibody to the β subunit of the receptor with high affinity for immunoglobulin E. Mol. Immunol. 25:647–661.
36. Rudolph, A. K., P. D. Burrows, and M. R. Wabl. 1981. Thirteen hybridomas secreting hapten-specific immunoglobulin E from mice with Igᵃ or Igᵇ heavy chain haplotype. Eur. J. Immunol. 11:527–529.
37. Saitoh, S., R. Arudchandran, T. S. Manetz, W. Zhang, C. L. Sommers, P. E. Love, J. Rivera, and L. E. Samelson. 2000. LAT is essential for FcεRI-mediated mast cell activation. Immunity 12:525–535.
38. Sheets, E. D., D. Holowka, and B. Baird. 1999. Critical role for cholesterol in Lyn-mediated tyrosine phosphorylation of FcεRI and their association with detergent-resistant membranes. J. Cell Biol. 145:877–887.
39. Shenoy-Scaria, A. M., L. K. Gauen, J. Kwong, A. S. Shaw, and D. M. Lublin. 1993. Palmitylation of an amino-terminal cysteine motif of protein tyrosine kinases p56^lck and p59^fyn mediates interaction with glycosyl-phosphatidylinositol-anchored proteins. Mol. Cell. Biol. 13:6385–6392.
40. Simons, K., and E. Ikonen. 1997. Functional rafts in cell membranes. Nature 387:569–572.
41. Song, J. S., J. Gomez, L. F. Stancato, and J. Rivera. 1996. Association of a p95 Vav-containing signaling complex with the FcεRI γ chain in the RBL-2H3 mast cell line. Evidence for a constitutive in vivo association of Vav with Grb2, Raf-1, and ERK2 in an active complex. J. Biol. Chem. 271:26962–26970.
42. Stauffer, T. P., and T. Meyer. 1997. Compartmentalized IgE receptor-mediated signal transduction in living cells. J. Cell Biol. 139:1447–1454.
43. Surviladze, Z., L. Dráberová, L. Kubínová, and P. Dráber. 1998. Functional

heterogeneity of Thy-1 membrane microdomains in rat basophilic leukemia cells. Eur. J. Immunol. **28:**1847–1858.

44. **Surviladze, Z., L. Dráberová, M. Kovářová, M. Boubelík, and P. Dráber.** 2001. Differential sensitivity to acute cholesterol lowering of activation mediated via the high-affinity IgE receptor and Thy-1 glycoprotein. Eur. J. Immunol. **31:**1–10.

45. **Swann, P. G., S. Odom, Y.-J. Zhou, Z. Szallasi, P. M. Blumberg, P. Draber, and J. Rivera.** 1999. Requirement for a negative charge at threonine 60 of the FcRγ for complete activation of Syk. J. Biol. Chem. **274:**23068–23077.

46. **Tolar, P., L. Dráberová, and P. Dráber.** 1997. Protein tyrosine kinase Syk is involved in Thy-1 signaling in rat basophilic leukemia cells. Eur. J. Immunol. **27:**3389–3397.

47. **Turner, H., K. Reif, J. Rivera, and D. A. Cantrell.** 1995. Regulation of the adapter molecule Grb2 by FcεR1 in the mast cell line RBL2H3. J. Biol. Chem. **270:**9500–9506.

48. **Vonakis, B. M., H. Chen, H. Haleem-Smith, and H. Metzger.** 1997. The unique domain as the site on Lyn kinase for its constitutive association with the high affinity receptor for IgE. J. Biol. Chem. **272:**24072–24080.

49. **Vonakis, B. M., H. Haleem-Smith, P. Benjamin, and H. Metzger.** 2001. Interaction between the unphosphorylated receptor with high affinity for IgE and Lyn kinase. J. Biol. Chem. **276:**1041–1050.

50. **Wilson, B. S., J. R. Pfeiffer, and J. M. Oliver.** 2000. Observing FcεRI signaling from the inside of the mast cell membrane. J. Cell Biol. **149:**1131–1142.

51. **Xavier, R., T. Brennan, Q. Li, C. McCormack, and B. Seed.** 1998. Membrane compartmentation is required for efficient T cell activation. Immunity **8:**723–732.

52. **Zhang, W., J. Sloan-Lancaster, J. Kitchen, R. P. Trible, and L. E. Samelson.** 1998. LAT: the ZAP-70 tyrosine kinase substrate that links T cell receptor to cellular activation. Cell **92:**83–92.

53. **Zhang, W., R. P. Trible, and L. E. Samelson.** 1998. LAT palmitoylation: its essential role in membrane microdomain targeting and tyrosine phosphorylation during T cell activation. Immunity **9:**239–246.